Effect of cavitation conditions on amorphous metal synthesis

M.W. Grinstaff, A.A. Cichowlas, S.-B. Choe and K.S. Suslick

School of Chemical Sciences, University of Illinois at Urbana-Champaign, 505 S. Mathews Avenue, Urbana, IL 61801, USA

Acoustic cavitation is an effective means of concentrating energy and can be used to drive a variety of chemical reactions. By changing the experimental parameters that control conditions during bubble collapse, different chemical environments can be created. The sonochemical reactions associated with metal carbonyls in alkane solvents are quite diverse and illustrate this phenomena. For example, ultrasonic irradiation of iron pentacarbonyl ($Fe(CO)_5$) under weak cavitation conditions initiates ligand substitution and cluster formation reactions. In contrast, under conditions that maximize the cavitational heating (for example, Ar, low vapour pressures, low ambient temperatures), the primary $Fe(CO)_5$ reaction is metal powder formation. The powder synthesized during sonolysis is amorphous and has unusual magnetic and catalytic properties. This amorphous iron powder is formed from the enormous heating and cooling rates generated during acoustic cavitation.

Keywords: sonochemistry; cavitation; amorphous metal synthesis

Acoustic cavitation is the physical phenomenon principally responsible for sonochemistry. By controlling cavitation conditions, one can tailor the chemical reactivity that occurs during ultrasonic irradiation of liquids. Our work on the sonochemistry of metal carbonyls illustrates this approach and will be discussed here. Our recent extension of this methodology has created a new and simple synthesis of an amorphous metal glass by the sonochemical decomposition of a volatile inorganic complex.

Acoustic cavitation

The chemical effects of ultrasound do not originate from a direct coupling of the acoustic field with the molecular species. Instead, they come from non-linear acoustic phenomena, primarily acoustic cavitation. Acoustic cavitation can be divided into three discrete stages: (1) formation, (2) growth and (3) implosive collapse[1-6].

Flynn proposed two types of cavitation: (1) stable cavitation, in which a bubble oscillates many times about its equilibrium radius with small excursions, and (2) transient cavitation, in which a short lived bubble undergoes dramatic volume changes in a few acoustic cycles and terminates in a violent collapse[5]. Both stable and transient cavitation may occur simultaneously in a solution, and a bubble undergoing stable cavitation may become a transient cavity[6].

Bubble formation is a nucleated process, and the nucleation sites are often gas-filled crevices in small particles suspended in solution (for example dust)[7]. Without these inhomogeneities in the liquid, the tensile strength of pure liquid would be ≈ 1000 atmospheres. Experimentally, however, we know that bubbles can be formed in a liquid with an expansion pressure wave of only a few atmospheres. Procedures that remove the particulates or their gas-filled crevices (such as exhaustive microfiltration, hydrostatic pressurization, or vacuum degassing) can dramatically increase cavitation thresholds.

Once formed, a bubble in an acoustic field can grow by several processes. At low acoustic pressures, rectified diffusion is important[6-8]. The bubble grows as dissolved gas enters during the expansion phase of the sound wave, and it shrinks during the compression phase. Since gas diffusion is dependent on surface area, slightly more gas enters the bubble than exits. Thus, the bubble will grow slowly over many acoustic cycles. In strong acoustic fields, the bubble oscillations can become very large through inertial effects. Rapid growth of a bubble during the expansion phase can have sufficient inertia to prevent the bubble from shrinking during the next compression wave.

In general, when a gas is compressed, it heats up. Bubbles growing into resonance size are well coupled to the sound field and can rapidly over-expand. At this point, rapid compression and consequent heating can occur. When the compression is rapid enough, the heating is nearly adiabatic: there is insufficient time for thermal transport to occur effectively. The ultrasonic irradiation of liquids produces localized 'hot-spots' that can initiate chemical reactions.

Factors affecting cavitation conditions

Because sonochemistry derives from this process of cavitation,

experimental parameters that affect the process of cavitation will alter the observed sonochemical reactions. Different chemical environments can be experimentally obtained by changing the conditions of the bubble collapse. These bubbles contain dissolved gases and solvent vapour.

Several properties of the gas in the bubble have dramatic effects on the bubble collapse[1,9-11]. One experimental parameter that is observed to alter sonochemical reactivities is γ, the ratio of C_p/C_v. γ determines the temperature increase of a gas during compression; it is a measure of the number of internal degrees of freedom. Monatomic gases have the highest γ (1.67) and give the highest temperatures; polyatomic gases can have γ approaching 1.0 and give little heating.

Another factor that affects bubble collapse is the thermal conductivity of the gas. If cavitation were completely adiabatic, helium and argon should have the same final temperature (the γ values are 1.67). In fact, helium dramatically decreases the rates of most observed sonochemical and sonoluminescence processes. The thermal conductivity differences for helium and argon (helium, $0.149\ W\ m^{-1}\ K^{-1}$; argon, $0.0172\ W\ m^{-1}\ K^{-1}$) account for much of this observed reactivity difference. The gas with the higher thermal conductivity reduces the adiabaticity of the collapse and lowers the peak temperature reached.

In sonochemical reactions, the bubble often contains not only a gas but a solvent vapour. Solvent molecules in the vapour phase have a low γ, which decreases the maximum cavitational temperature. In addition, the solvent vapour in the bubble is compressible, which also strips energy away from the adiabatic heating[12]. Furthermore the solvent molecules in the bubble can undergo their own sonochemical reactions, removing energy from the bubble and decreasing the temperature reached during cavitation[13]. Thus, as more volatile solvents are used, the effective temperature reached during bubble collapse is lower.

Temperature of cavitation

Since the early calculations of Lord Rayleigh, the temperature of cavitation has been predicted to be in the thousands of degrees[14]. In the late 1980s, Suslick, Cline and Hammerton experimentally measured the temperature reached during cavitation[15]. Using comparative rate thermometry they determined that there are two sites of chemical reactivity during bubble collapse. The first region is initially gas-phase, presumably within the cavitating bubble, and has an associated temperature of $5200 \pm 650\ K$ for cavitation at 20 kHz under Ar in alkanes with a vapour pressure of 5 torr. The second region is liquid-phase before collapse, which may correspond to either the shell of the liquid around the collapsed bubble or to small droplets of liquid splattered into the collapsing bubble by surface wave activity; this second reaction zone has an effective temperature of $\approx 2000\ K$. This comparative rate thermometry experiment provided information about the temperature based upon previously known chemical reactivities.

Very recently, Suslick and Flint have determined from sonoluminescence spectra the emission temperature of excited state molecules produced during cavitation[16]. Emission from the Swan band of $C_2(d^3\Pi_g \rightarrow a^3\Pi_u)$ is seen during ultrasonic irradiation of many organic liquids, including silicon oil (polydimethylsiloxane). The temperature was experimentally determined by modelling the individual rotational vibrational transitions of the Swan band. The best computational fit to the raw data is at an emission temperature of $5080 \pm 160\ K$, at 20 kHz under Ar in silicone oil with a vapour pressure of ≈ 0.01 torr. The measurement of the Swan-band emission temperature represents only the effective temperature of C_2 in the $d^3\Pi_g$ excited state, and not necessarily that of other species created during the cavitation event.

We wish to emphasize that there can be no single temperature to describe all species present during cavitation. The local conditions in a cavitating bubble are extraordinarily dynamic, both spatially and temporally. The spatial and temporal temperature profile of a cavitating bubble remains an important question that has not yet been resolved. The application of time-resolved measurements of a single cavitating bubble may prove especially useful in providing a full profile of the cavitation event.

Hot-spot lifetime

Recently, Barber and Putterman measured the lifetime of bubble collapse for a single bubble undergoing *stable* cavitation in a 20 kHz acoustic field[17]. Monitoring the sonoluminescence from a single bubble, they determined that bubble collapse occurs in less than 100 ps. Further experiments in their laboratory suggested that the lifetime of the emission is actually less than 50 ps (personal communication). This lifetime is several orders of magnitude shorter than previous reports of Margulis[18-20] and Benkovskii[21] who have suggested that the lifetime ranges from 5 ns to 5 ms.
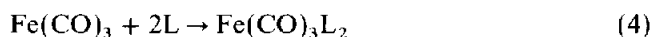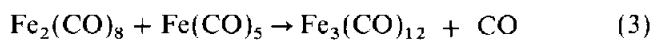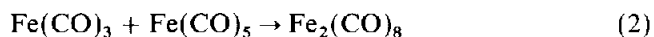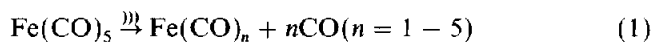
These sonoluminescence flashes or 'bursts' contain more than 10^5 photons. Acoustic cavitation converts the diffuse energy of the sound wave into a concentrated energy burst with a lifetime of picoseconds. The mechanism responsible for the very short length of this emission remains open.

The sonochemistry of metal carbonyls

The sonochemical reactions associated with the ultrasonic irradiation of metal carbonyls in alkane solvents are quite diverse and are strongly influenced by the cavitation conditions. Among the various sonochemical reactions observed are ligand substitution, ligand loss and metal–metal bond formation to produce multi-metallic cluster complexes, and initiation of alkene isomerization. Our underlying goal is to introduce enough energy into the metal carbonyl to initiate reaction, but to do so in a controlled and selective manner.

Most simple metal carbonyls, including $Fe(CO)_5$, $Cr(CO)_6$, $Mo(CO)_6$, $W(CO)_6$, and $Mn_2(CO)_{10}$ are sonochemically active[22]. The sonochemical reactivities of these metal carbonyls are strongly controlled by the cavitation conditions. Our previous work on the effect of vapour pressure on the sonochemical reactions of $Fe(CO)_5$ illustrates this point[22-25]. At high solvent vapour pressure (that is, low cavitational temperature), the major reactions that occur are ligand substitution and cluster formation as shown in (1)–(4). Under conditions that maximize the cavitational heating (low vapour pressure and Ar dissolved gas), the loss of multiple CO ligands dominates (1), and clusterfication is replaced

by metal formation. The ratio of yields of Fe to $Fe_3(CO)_{12}$ decrease from approximately 50 to 0.25 as the solvent vapour pressure increases from decane through heptane. As discussed below, we have recently discovered that the iron powder so produced is *amorphous* and may have important technological applications[26,27].

$$Fe(CO)_5 \xrightarrow{))} Fe(CO)_n + nCO(n = 1 - 5) \qquad (1)$$

$$Fe(CO)_3 + Fe(CO)_5 \rightarrow Fe_2(CO)_8 \qquad (2)$$

$$Fe_2(CO)_8 + Fe(CO)_5 \rightarrow Fe_3(CO)_{12} + CO \qquad (3)$$

$$Fe(CO)_3 + 2L \rightarrow Fe(CO)_3L_2 \qquad (4)$$

This sonochemical reactivity is contrasted with the thermal and photochemical reactivities of $Fe(CO)_5$. Of special note is the sonochemical synthesis of $Fe_3(CO)_{12}$ from intermediates with multiple CO losses. Such intermediates were confirmed by ligand substitution studies ((4), where L = phosphines, phosphites or amines). The primarily ligand substitution products formed are $Fe(CO)_4L$ and $Fe(CO)_3L_2$, which are indicative of coordinated unsaturated intermediates. In contrast, multiple ligand loss is not easily available from simple bulk heating or photolysis, and $Fe_3(CO)_{12}$ is not formed directly. Thermolysis of $Fe(CO)_5$ produces crystalline iron powder, and ultra-violet photolysis yields $Fe_2(CO)_9$.

The sonochemical synthesis and characterization of amorphous iron

If a molten metal is cooled sufficiently rapidly, the liquid will solidify before crystallization can occur. The resulting material is a super-cooled liquid, an amorphous metal alloy. These 'metallic glasses' lack long range crystalline order in their structure. Amorphous metal alloys are presently formed by splattering molten metal on a cold surface using techniques such as roller or splat quenching[28]. These techniques must generate cooling rates of $\approx 10^5$ to $10^7 K s^{-1}$, and are consequently experimentally difficult and expensive. In addition, large amounts of other alloying elements (for example, $> 20\%$ C, B, Ni etc) are necessary additives to help prevent crystallization during cooling[29,30]. The effort is worthwhile, however, because amorphous metals have many important industrial applications, including corrosion resistant coatings, power transformer cores, magnetic storage media, and cryothermometry[28-30].

We have discovered a new synthetic route to metallic glass powders making use of the extreme conditions created by high intensity ultrasound. As described earlier, the effective temperature reached during bubble collapse is ≈ 5000 K with submicrosecond lifetimes. Thus, we predict the heating and cooling rates during cavitational collapse to be $> 5 \times 10^6 K s^{-1}$ (and if the hot-spot lifetime were as short as the sonoluminescence pulse, $\approx 5 \times 10^{11} K s^{-1}$). Acoustic cavitation might therefore provide a new route to amorphous metals. By using volatile metal containing compounds, and decomposing them sonochemically, we hypothesized that ultrasonic irradiation could produce relatively pure metallic glasses. Along these lines, we have recently observed iron atomic emission lines during ultrasonic irradiation of iron pentacarbonyl, a volatile organometallic compound, thus confirming the formation of iron atoms during cavitation[31].

Ultrasonic irradiation of 4.0 M decane solutions of $Fe(CO)_5$ yields a dull black powder in gram quantities[26-27]. The irradiation was accomplished at $0 °C$ with a high intensity ultrasonic probe (Sonics and Materials, model VC-600, 0.5 in Ti horn, 20 kHz, $100 W cm^{-2}$) for 3 h under argon. The iron powder produced was filtered after irradiation and washed with dry pentane in an inert atmosphere box (Vacuum Atmospheres, < 1 ppm O_2). The iron powder proved to be relatively pure, compared with splat-cooled amorphous alloys. Elemental analysis showed $> 96\%$ iron by weight, with a trace amount of carbon (3%) and oxygen (1%), presumably from the decomposition of alkane solvent or carbon monoxide during ultrasonic irradiation.

The iron powder was characterized with a variety of measurements. Scanning electron micrographs of the sonochemically synthesized iron powder show conchoidal fractures, which are typical for non-crystalline materials (*Figure 1*). At higher magnification, the scanning electron micrographs show that the bulk material is a composite of many smaller iron particles (*Figure 2*). A transmission electron micrograph of the amorphous iron is shown in *Figure 3*, confirming the agglomerated nature of the solid. After long exposure to heating from the electron beam, partial crystallization occurs *in situ* in the electron microscope. *Figure 4* shows the formation of ≈ 40 nm crystallites during such crystallization. Both the scanning and transmission electron micrographs reveal the powder to be porous agglomerates of very small particles.

The non-crystalline nature of this material was established by several techniques. A large exothermic

Figure 1 Low resolution scanning electron micrograph of amorphous iron powder produced from ultrasonic irradiation of $Fe(CO)_5$ (Hitachi S800)
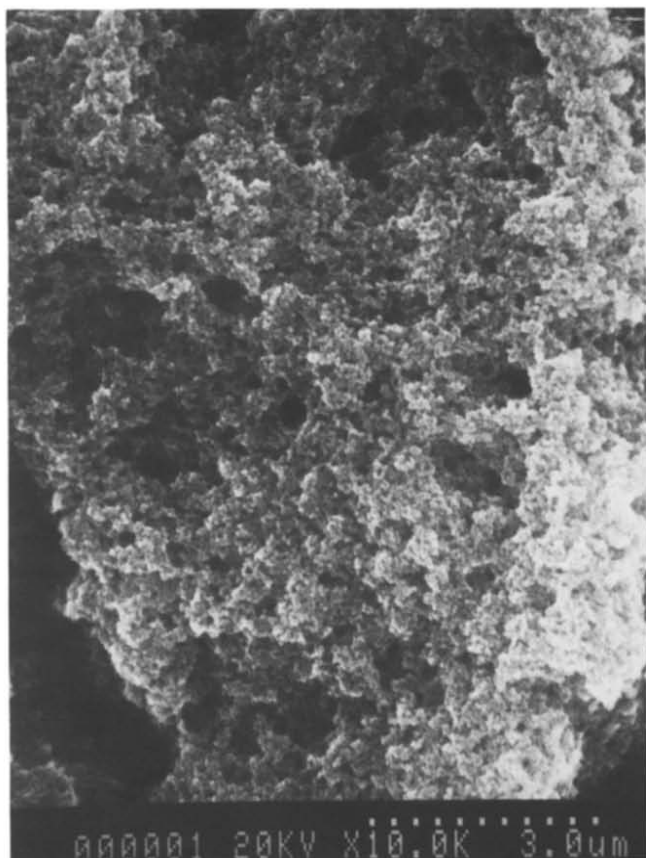
Figure 2 High resolution scanning electron micrograph of amorphous iron powder produced from ultrasonic irradiation of $Fe(CO)_5$ (Hitachi S800)
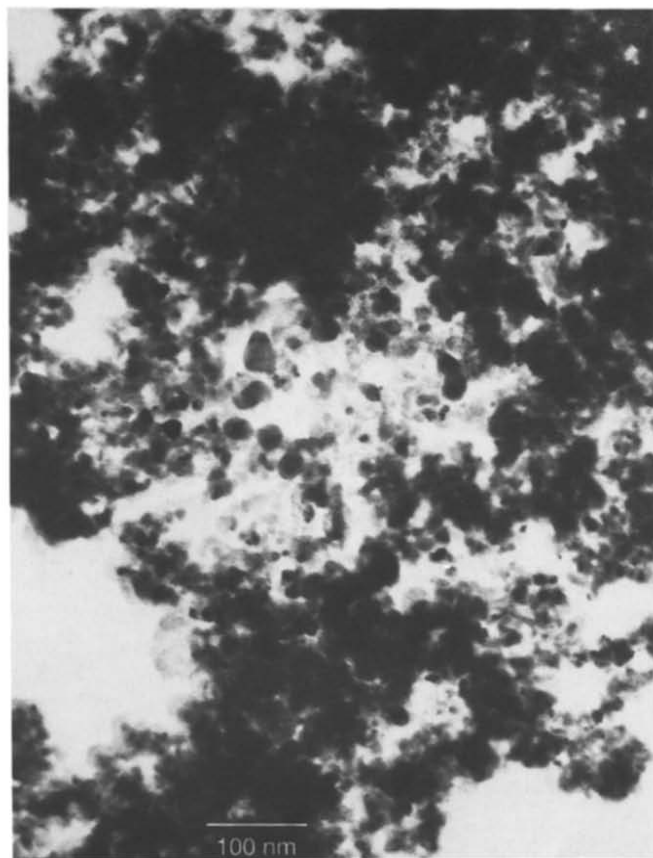

Figure 4 Transmission electron micrograph of iron powder after crystallization has occurred from electron beam heating *in situ* (Philips EM 400T)

Figure 3 Transmission electron micrograph of amorphous iron powder before crystallization (Philips EM 400T)

transition at 308 °C corresponding to a disorder/order transition (that is, crystallization) of the amorphous iron is observed in the differential scanning calorimetry (DSC) scan. Crystalline iron purchased from Aldrich as well as heat-treated amorphous iron shows no DSC transitions. Transmission electron microdiffraction experiments confirm the DSC data and show only a diffuse ring characteristic of an amorphous material. After continued sample exposure in the electron beam, the iron powder crystallizes *in situ* and the diffraction rings from α-Fe are observed. The crystallization of the amorphous iron to α iron was also confirmed using X-ray powder diffraction, as shown in *Figure 5*. The initial diffraction pattern shows no diffraction peaks and, upon heating, the lines characteristic of α-iron metal (d Å: 2.03, 1.43, 1.17, 1.04) are observed.

The surface area of the amorphous iron was determined by BET gas adsorption and found to be $120 \, \text{m}^2 \, \text{g}^{-1}$. This surface area is ≈ 150 times greater than commercially available ultrafine, crystalline iron powder ($5 \, \mu\text{m}$ diameter, Aldrich Chemicals) and contributes to its very high chemical reactivity (for example, it is pyrophoric). The high surface area measurement by BET agrees qualitatively with the SEM and TEM data. Surprisingly, the sonochemically-produced amorphous iron powder sinters at unusually low temperatures. The surface area reduces to $< 10 \, \text{m}^2 \, \text{g}^{-1}$ at 300 °C. The amorphous iron powder is a reactive catalyst for the hydrogenolysis and dehydrogenation of saturated hydrocarbons[26,27]; it is ≈ 100 times more reactive than the ultrafine crystalline iron powder on a mass basis.
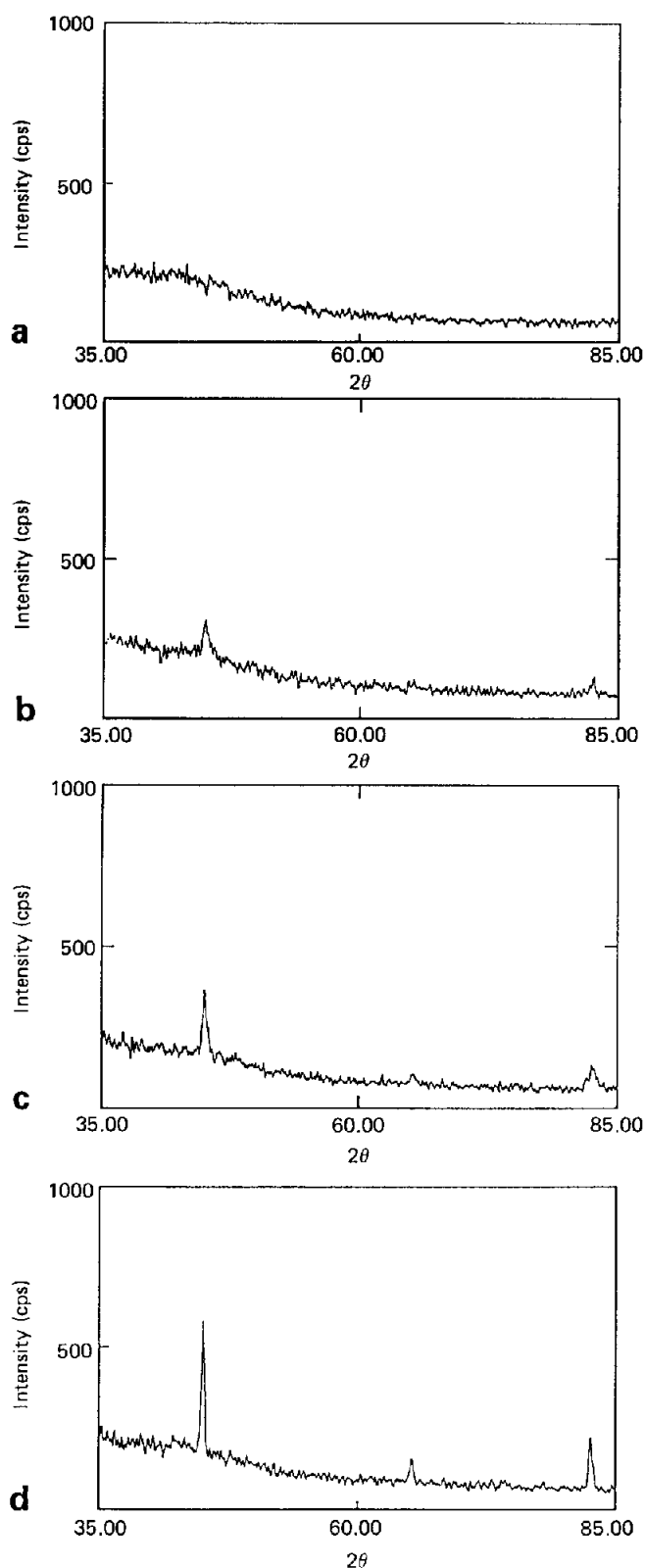
Figure 5 X-ray powder diffraction powder of amorphous iron (Rigaku D-max diffractometer). (a) Before heat treatment; (b) heated under N_2 at 200 °C for 6 h; (c) heated under N_2 at 300 °C for 6 h; (d) heated under N_2 at 350 °C for 6 h

In summary, the conditions of cavitation can be tailored to produce specific chemical reactions. The reactions of organometallic complexes provide an important example. Ligand substitution and metal cluster formation occur at high vapour pressures. In contrast, at low vapour pressure where the cavitation collapse is most severe, amorphous iron metal is synthesized.

Acknowledgements

References

1 Suslick, K.S. (Ed) *Ultrasound: Its Chemical, Physical and Biological Effects* VCH Publishers, New York (1988)
2 Suslick, K.S. *Science* (1990) **247** 1439
3 Suslick, K.S. *Sci Am* (1989) **260** 80
4 Mason, T.J. (Ed) *Sonochemistry: The Uses of Ultrasound in Chemistry* Royal Society of Chemistry, Cambridge, UK (1990)
5 Flynn, H.G., in: *Physical Acoustics* Vol IB (Ed Mason, W.P.) Academic Press, New York, (1964) 57
6 Apfel, R.E., in: *Methods of Experimental Physics: Ultrasonics* (Ed Edmonds, P.D.) Academic Press, New York (1981)
7 Atcheley, A.A., Crum, L.A., in: *Ultrasound: Its Chemical, Physical and Biological Effects* (Ed Suslick, K.S.) VCH Publishers, New York (1988)
8 Crum, L.A. *J Acoust Soc Am* (1982) **72** 1568
9 Suslick, K.S., Doktycz, S.J., Flint, E.B. *Ultrasonic* (1990) **28** 280
10 Yong, F.R. *J Acoust Soc Am* (1976) **60** 100
11 Prudhomme, R.O., Guilment, Y. *J Chem Phys* (1957) **54** 336
12 Fujikawa, S., Akamatsu, T. *J Fluid Mech* (1980) **97** 481
13 Fogler, S. *Can J Chem Eng* (1969) **47** 242
14 Lord Rayleigh *Phil Mag* (1917) **34** 94
15 Suslick, K.S., Cline, R.E. Jr., Hammerton, D.A. *J Am Chem Soc* (1986) **108** 5641
16 Flint, E.B., Suslick, K.S. *Science* (1991) **253** 1397
17 Barber, B.P., Putterman, S.J. *Nature* (1991) **352** 318
18 Margulis, M.A. *Sov Phys Acoust* (1991) **22** 310
19 Kurochkin, A.K., Smoradov, E.A., Valitov, R.V., Margulis, M.A. *Russian J Phys Chem* (1986) **60** 731
20 Margulis, M.A., Dmitrieva, A.F. *Russian J Phys Chem* (1982) **56** 198
21 Benkovskii, V.G., Golobnichii, P.I., Olzoev, K.F. *Sov Phys Acoust* (1974) **20** 74
22 Suslick, K.S. *Adv Organomet Chem* (1986) **25** 73
23 Suslick, K.S., Schubert, P.F., Goodale, J.W. *J Am Chem Soc* (1981) **106** 7324
24 Suslick, K.S., Goodale, J.W., Wang, H.H., Schubert, P.F. *J Am Chem Soc* (1983) **105** 5781
25 Suslick, K.S., Schubert, P.F. *J Am Chem Soc* (1983) **105** 6042
26 Suslick, K.S., Choe, S.B., Cichowlas, A.A., Grinstaff, M.W. *Nature* (1991) **353** 414
27 Suslick, K.S., Choe, S.B., Cichowlas, A.A., Grinstaff, M.W. *US Patent Application* 25 Sept. (1991)
28 Takayama, S. *J Mat Sci* (1976) **11** 164
29 Anatharaman, T.R. *Metallic Glasses* Trans Tech Publication: Aedermannsdorf, Switzerland (1984)
30 Steeb, H., Warlimont, H. (Eds) *Rapidly Quenched Metals* Elsevier Science, Amsterdam (1985)
31 Suslick, K.S., Flint, E.B., Grinstaff, M.W., Klemper, K.A. To be submitted